Seeing the piles of the velvet bending under our finger sliding over a tactile stimulator improves the feeling of the fabric

Laurence Mouchnino, Brigitte Camillieri, Jenny Faucheu, Mihaela Juganaru, Alix Moinon, Jean Blouin, Marie-Ange Bueno

Paper published in the Journal *of the Royal Society Interface 21(220), 20240368* and freely available at https://www.researchgate.net/profile/Jean-Blouin-3/research

Seeing the piles of the velvet bending under our finger sliding over a tactile stimulator improves the feeling of the fabric

Laurence Mouchnino[1,2], Brigitte Camillieri[3], Jenny Faucheu[4], Mihaela Juganaru[5], Alix Moinon[1], Jean Blouin[1], Marie-Ange Bueno[3]

[1] Aix Marseille Univ, CNRS, Centre de Recherche en Psychologie et Neurosciences, Marseille, France

[2] Institut Universitaire de France, Paris

[3] Université de Haute-Alsace, Laboratoire de Physique et Mécanique Textiles (UR 4365), École Nationale Supérieure d'Ingénieurs Sud Alsace, Mulhouse, France

[4] Mines Saint-Etienne, Univ. Lyon, CNRS, UMR 5307 LGF, Saint-Etienne, France

[5] Mines Saint-Etienne, Institut Henri Fayol, Département ISI, Saint-Etienne, France

Abstract

Using friction modulation to simulate fabrics with a tactile stimulator (i.e. virtual surface) is not sufficient to render fabric touch and even more so for hairy fabrics. We hypothesized that seeing the pile of the velvet darken or lighten depending on changes in the finger movement direction on the virtual surface should improve the velvet fabric rendering. Participants actively rubbed a tactile device or a velvet fabric looking at a screen that showed a synthesized image of a velvet which either remained static (V-static) or darkening/lightening with the direction of touch (V-moving). We showed that in V-moving condition, the touched surface was always perceived rougher, which is a descriptor of a real velvet (*Experiment 1*). Using electroencephalography and sources localization analyses, we found increased activity in the occipital and inferior parietal lobes (*Experiment 2*) when seeing dark and shinning traces during back and forth finger movements over the virtual surface. This suggests that these two posterior cortical regions work together to evaluate visuo-tactile congruence between the seen and the felt (tactile). The visuo-tactile binding, evidenced by neural synchronization (specifically, theta band [5-7 Hz] oscillation) in the left inferior posterior parietal lobule, is consistent with enhanced integration of information and likely contributed to the emergence of a more realistic velvet representation.

3-6 key words: Tactile, EEG, Friction, Finger movement, Perception, Tactile device

1. Introduction

Most of our daily interactions with the environment are based on goal-directed movements to explore and perceive materials or objects. This is mainly done by tactile exploration using the glabrous skin areas of the hand or foot. During this process, the brain actively modulates movement parameters, such as the contact force between the skin and the surface, the movement velocity and its direction. Meanwhile, the skin of the body segment in contact with the surface undergoes deformation during the motion thereby stimulating the tactile receptors. For example, microneurography recordings showed greater responses of both fast-adapting (FA) and slow-adapting (SA) tactile receptors (i.e., enhanced number and frequency of the spikes) when the direction of the movement of the finger in contact with hairy textile materials was against the main pile direction, as compared to along the pile direction (Breugnot et al., 2006). At first sight, what seems relevant for discriminating textures are the properties of the surfaces in contact (i.e., the skin of the hand and the materials) together with their relative motion. The friction-induced vibrations (i.e. FIV) that propagate in the skin during motion are also particularly relevant for the perception of fine textures (Faucheu et al., 2019; Manfredi et al., 2014; Massimiani et al., 2020). The vibration and the FIV would be mainly detected through Pacinian receptors (i.e. FAII), which are exquisitely sensitive to vibration (~100-300 Hz, Johansson and Vallbo, 1983). However, finger-surface interactions do not only engage these receptors as FIV also stimulates fast- and slow-adapting receptors providing a rich and complex composition of tactile information (e.g., FAI, SAI and SAII, Dione et al., 2021).

Conceptually, the fact that fabrics discrimination strongly relies on friction modulation in a large frequency bandwidth from 0 to approximately 1000 Hz opens the possibility of creating devices capable of simulating different fabrics. Indeed, textiles have a minimal spatial period of some tens of microns and stimulators with friction modulation are good candidates to emulate fabrics (Bueno et al., 2014; 2015). The challenge is to give the illusion of touching a real fabric when exploring a tactile feedback device. Devices capable of reproducing surfaces have been designed by different groups using different technologies (e.g., Biet et al., 2008; Felicetti et al., 2022). Using ultrasonic vibrations to modulate the coefficient of friction between the finger and the surface, the STIMTAC device has been used in several tribology studies (Biet et al., 2008; Bueno et al., 2014; 2015; Camillieri et al., 2018). This device has proved to be interesting for reproducing textile fabric. Psychophysical investigations using the STIMTAC tactile device have shown that the perceptual rendering is promising (Weiland et al., 2024) but presents some limits in particular for hairy fabric (velvet) (Camillieri et al., 2018; Bueno et al., 2015). This

perceptual discrepancy when touching real and simulated velvet could be partly due to the fact that the power of the respective FIV in the bandwidth [100–400 Hz] differed greatly (Camillieri et al., 2018). For instance, creating virtual textured surfaces by generating patterns of sliding and braking sensations by adjusting the vibration amplitude of the wave as the finger, equipped with a position sensor, moves on the surface (Biet et al. 2008) reliably created virtual twill fabric but failed to simulate very hairy surfaces such as velvet fabric (Camilieri et al. 2018). In addition, the response of the SAI units to the skin indentation (Merkel endings, Harrington and Merzenich, 1970) that should be produced when the finger is moving against the pile of the velvet, is lacking when contacting a tactile device.

Although the material qualities are mainly estimated by the sense of touch, the visual system is capable of providing rough information about material properties even before touching it (Tiest and Kappers, 2007; Baumgartner et al., 2013). For instance, the view of a surface with long curled hairs (like angora rabbit) is likely to be judged softer than a surface with short bristly hairs. Notably, the visual perception of the surface roughness is greatly dependent on the illumination direction: observers perceive surfaces to be markedly rougher with decreasing illuminant angle (Ho et al., 2006). Seeing how a surface is transformed when touching it can also provide information about the properties and identity of the surface such as compliance and friction (see Ujitoko and Ban 2021, for a review). According to the current understanding of the weighting of visual and tactile feedbacks for perceiving such object properties, the brain uses estimates of the reliability (i.e., variance estimate) of each sensory modality to determine their respective contribution (Ernst and Banks 2002). The lower the variance estimate of a sensory modality, the higher the contribution of that modality. For instance, in contexts where tactile stimulation is less reliable (“noisy” stimulus), seeing dark and shinning traces during back and forth finger movements over the surface is likely to evoke the perception of a velvet-like fabric (a feature well exploited by painters such as Rembrandt who depicted the velvet fabric's soft folds and luxurious sheen in the “Old man with beard, fur cap, and velvet cloak”). A possible mechanism underlying this phenomenon is that the view of the physical consequences of our interaction with these fabrics, would reactivate stored internal representations of the fabric properties that have been constructed during previous active explorations with the fabric (e.g., Romo et al., 2003; Zhou and Fuster, 2000).

The above-mentioned effects of visual information suggest that, during finger exploration, the appraisal of the surface properties might differ in contexts with and without surface-related visual feedback (see Driver and Spence, 2000 for a review). The various areas where tactile and

visual sensory inputs converge in the brain could permit the visual inputs to influence tactile perception. This includes areas dedicated to the early (e.g., primary somatosensory cortex, Dionne et al., 2010; Zhou and Fuster, 2000) and subsequent stages of sensory processing (e.g., inferior premotor and inferior parietal cortex cortices; Sereno and Huang, 2014; Ishida et al., 2010). These brain areas contain cells that respond to either tactile or visual inputs, but also bimodal cells that respond to both tactile and visual stimulus. Internal representations and perceptual experience would be strongly contingent upon the activity of these regions. Hence, preventing the brain to be fueled with both visual and tactile inputs could limit the possibility of perceiving virtual fabrics through tactile devices.

In the present study, we tested the hypothesis that through sensory integration processes, immerging participants in a context that simulates finger friction/vibrations characterizing exploration of a velvet fabric, together with the visual (but virtual) consequence of the finger motion on velvet (i.e. shading/sheen changes) will improve the perception of the velvet. We used a twofold approach to test this hypothesis. First, the influence of the additional visual input on the perceptive attributes of simulated velvet fabric was analyzed through a behavioral study based on paired comparison tests *(Experiment 1)*. We used the exploratory procedure (motor activity) for extracting particular object properties with accuracy and/or speed judgement (Klatzky et al., 1989). Specifically, this procedure necessitated local pressure of the fingertip during the exploratory movement to provide more detailed properties (e.g., softness, thickness, relief) as Giboreau et al. (2001). Our second approach is based on the current consensus that functional processing of sensory inputs is associated with the modulation of band-specific neural oscillation power (Fabre et al., 2023; Haegens et al., 2011; Pfurtscheller and Lopes da Silva, 1999). Notably, ongoing oscillations would shape our perception. In particular, oscillations within the low frequency bands (theta and alpha) would be linked to perceptual functions, notably to the perception or non-perception of a stimulus (Busch et al., 2009; Busch and VanRullen, 2010). We predicted that combining visual and tactile information when moving the index finger on a tactile device simulating the friction between the finger and a velvet fabric will modulate theta and alpha powers in the inferior parietal cortex (PPC), a key region for processing of tactile (Haegens et al., 2011) and visuo-proprioceptive information *(Experiment 2)*.

2. *Experiment 1*: Perception

2.1 Materials and Methods

Twenty-two participants (9 women and 13 men) who did not have any known neurological, physiological, cognitive or motor disorders participated to the experiment (20 right-handed and 2 left-handed, mean age: 27 ± 4 years). The experiment was conducted with the understanding and written consent of each participant, and all procedures were approved by the CERSTAPS ethic committee (IRB00012476-2021-09-12-140). The protocol and procedure adhered to the guidelines established in the 1964 Declaration of Helsinki. All participants will be able to stop the study at any time of their own accord or following the decision of the experimenter. None of the participants had participated in any similar previous experiments.

The experiment took place in a room with conditioned atmosphere (20 ± 2°C and 65 ± 5% of relative humidity). Before each experiment, the participants washed and dried their hands. During the experiment, the participants were seated in front of a table on which the STIMTAC tactile device was positioned. A computer screen was located 40 cm behind the device. An adjustable support covered with a towel held the subject's arm in a correct and comfortable position. The hand and the exploring surface were occluded from view by a custom-made box (Fig. 1). The STIMTAC is able to simulate different fabric-like materials (Ben Messaoud et al., 2016, Weiland et al. 2024) by inducing ultrasonic vibrations (at a constant value between 30-40 kHz) of the device surface relative to the finger position (Biet et al., 2008). Changing the amplitude of the vibration allows modulating the coefficient of friction (COF) between the finger and the surface, which is a key parameter for discriminating textures (Manfredi et al., 2014). With velvets (in particular pane velvet) the sensation of rubbing against the nap is very different to rubbing with the nap. To this end the STIMTAC coordinates the vibrations depending on the direction of movement to reinforce the sensation of a real velvet (Camilieri et al. 2018).

In the present study, the STIMTAC generated two different tactile stimuli to simulate two different percepts. The virtual velvet tactile stimulus reproduced the friction recording during exploration of velvet (as in Camillieri et al., 2018) while the virtual sham tactile stimulus is generated from virtual velvet but with a lower magnitude, corresponding to no known fabrics. More specifically, the vibration amplitude used to generate the virtual velvet stimulus was set at 74% of the STIMTAC's maximum vibration amplitude, while the vibration amplitude of the virtual sham stimulus was set at 0.57* virtual velvet. Note that the measured mean perception threshold of the vibrations across participants was 0.19* virtual velvet.

The computer screen presented a 12 x 10 cm synthesized image of grey velvet with a yellow dot on which the participants fixated throughout the trials (see Fig. 1). During the tactile exploration of the surface (see below), the visual display either remained static (V-static) or simulated the traces that would have been left if the participant's index finger was sliding on a real velvet fabric (V-moving). The STIMTAC device records the position of the finger enabling the visual display to be modified in real time. More specifically, when the participants rubbed the surface against the nap (or grain) of the simulated pile (i.e. towards the right in this protocol), the visual display left a dark trail (as if the velvet fibers straightened). When they rubbed the surface along the nap of the simulated pile (i.e. towards the leftward direction), the traces on the screen became lighter (as if the velvet fibers flattened). The spatiotemporal characteristics of the traces displayed on the screen matched those of the index finger movements on the STIMTAC surface (a crucial aspect for visuo-somatosensory integration, see Hidaka et al., 2015 for a review).

The participants were asked to produce back and forth lateral movements with the index finger to explore the stimuli programmed on the STIMTAC tactile stimulator. The mean amplitude and velocity of the sliding finger movements were ~40 mm and ~40 mm/s, respectively. A 1 Hz metronome beat helped the participants to achieve the desired movement velocity. The instructions specified that the normal force on the surface had to be ~0.5 N. Before the experimental session, the participants were trained to produce finger movements which complied with all these specifications. For this training session, two dots, 40 mm apart were positioned just in front of the exploring surface and a monitor provided the normal force feedback to the participants (see Fig. 1). During the training session, the finger movements were performed on a different fabric. Only a few back and forth movements were necessary for the participants to comply with the required movement features.

For the experiment, four different visuo-tactile stimuli were designed according to the selected combination of tactile (i.e., virtual velvet or virtual sham) and visual stimuli (i.e., V-static or V-moving) (see Table 1).

The task of the participants was to compare the roughness between the surfaces presented in two distinct sets of visuo-tactile stimuli. For each paired comparison test, the participants indicated "which surface is rougher"? The participants were instructed that they could answer that the two surfaces had the same roughness. The French term "râpeux" was selected for "rougher" among several French terms describing rough textures from Bassereau and Charvet-Pellot (2011). We chose this descriptor to describe the effect of the pile tuft under the fingers

which can well characterize the “velvet effect”, i.e. the difference between the feeling when moving the finger along and against the pile direction. At the beginning of the test, the participants explored the first presented visuo-tactile stimuli before exploring the second. They were allowed to explore each surface for as long and as many times as required. The order of presentation of the different visuo-tactile stimuli was based on a Latin square-like design allowing for 16 pairs randomly presented for each participant. Therefore, each visuo-tactile stimulus was presented as often in first and second positions. For the analyses, the pairs were categorized according to the sequence of their presentation. Each participant touched a sample of real velvet before starting the experiment, and at three moments equally spaced in time during the experiment to refresh the “velvet effect”.

2.2. Statistical analyses

In *Experiment* 1, for each paired comparison, based on the votes provided by all 22 participants, the frequency of occurrence of one visuo-tactile stimulus being perceived rougher is observed for each pair of stimuli. The $\chi 2$ Pearson's test for homogeneity is used to test the null hypothesis of having a frequency of votes deriving from chance alone. The results show a p value of 0.01133 (i.e., < 0.05) which means that the null hypothesis is rejected and the votes for paired comparison can be analyzed with regards of the effects of visual and tactile conditions on the perception of roughness.

2.3. Results

The overall analysis of the collected data showed evidence of a position bias which is commonly observed in paired comparison experiments (Penny et al., 1972; Day, 1969). The position bias is observed when considering all paired comparison results in that the vote count of all 22 participants shows that tactile stimuli presented in the second position are more often perceived rougher than stimuli presented in the first position 161 vs 110 votes, considering all the t votes. Interestingly, the position bias is observed for all comparisons between the same visuo-tactile stimuli, except for the comparison involving virtual velvet/V-moving *vs* virtual velvet/V-moving. In the former comparisons, the tactile stimuli presented in the second position are perceived (incorrectly) as rougher than the same stimuli presented in the first position. The observed frequency to take the second tactile stimulus as rougher is f_2=0.46 and the frequency

to take the first as rougher is f_I=0.31, both with a confidence interval of [f-0.05; f+0.05]. In the later comparison (virtual velvet/V-moving *vs* virtual velvet/V-moving), the stimuli are mostly perceived (correctly) as the same stimulus which tends to indicate that the tactile stimulus is more clearly perceived than in the three other visuo-tactile conditions.

To account for position bias, the collected data were analyzed with respect to the order of presentation using Bayesian methods. These methods establish a mathematical relationship between conditional probabilities that relates the posterior probability of parameter values on the one hand, to the probability of the data given the parameter values and the prior probability of the parameter values, on the other hand (Kruschke, 2010). The analysis focused in particular for pairs including virtual velvet/V-moving. The observed frequencies of tactile stimulus of virtual velvet/V-moving being perceived rougher than in another visuo-tactile stimuli when presented in either first or second position was calculated (Table 2). Relative to virtual sham/V-moving and virtual sham/V-static, tactile stimulus in virtual velvet/V-moving was perceived rougher when presented in both first and second position. The result was consistent with the fact that the tactile stimulus reproduced the FIV recorded when exploring real velvet (i.e., rough fabric) while in both virtual sham, the tactile stimulus reproduced only a fraction of the original signal (i.e., 57%). More importantly, the tactile stimulus in virtual velvet/V-moving relative to virtual velvet/V-static was also perceived rougher when presented in both first and second position. Remarkably, in this case, the vibration characteristics were exactly the same. The only difference was in the type of visual feedback associated with the explorative finger movements. This finding indicated that the visual feedback sharpened the roughness perception. It also suggested that, alone, the moving visual feedback provided during finger exploration had limited capacity to create the illusion that one was touching real velvet when associated to virtual sham tactile stimulus.

Observed frequencies such as those presented in Table 2 correspond to conditional probabilities, the condition is related to the presentation position (first or second). The frequencies of a response during a comparison are assimilated as probability of choosing a response for the first visuo-tactile stimuli of a pair. Using these choice probabilities, the Bayesian inference (Box & Tiao, 2011) allowed us to derive responses scores, see Table 3. The computation shows that virtual velvet/V-moving is identified as rougher than the 3 other visuo-tactile stimuli. Moreover, virtual sham/V-static is considered as less rough than the 3 other visuo-tactile stimuli.

3. *Experiment* 2: Tribological measurement and electroencephalography

3.1 Materials and Methods

The experiment was carried out with the same ethical and environmental conditions as in *Experiment* 1. Fourteen right-handed participants (10 women and 4 men, mean age: 27 ± 2 years) without any known neurological, physiological, cognitive and motor disorders participated in the experiment. None had participated in any previous similar experiments. The Semmes–Weinstein monofilament test was carried out to determine the sensibility of the index finger pad of each participant. The sensitivity thresholds varied between 0.023 g to 0.166 g (mean 0.11 grams ± 0.06) and were therefore deemed as 'normal' (Hage et al., 1995).

Because finger skin hydration can significantly influence friction and, consequently, tactile perception (Cornuault et al., 2015), we measured finger moisture for each participant using a Corneometer® CM825. We took five measurements: one before the experiment, one at the end, and three during the experiment. Consistent with findings from a similar experiment (i.e., Weiland et al., 2024), our study showed no significant change in skin hydration over the course of the experiment (mean standard deviation of 9 a.u.). Across all participants, skin hydration ranged from 42 to 103 a.u., with a mean of 63 a.u.

The same set-up as in *Experiment* 1 was used in *Experiment* 2 (e.g., computer screen, STIMTAC device) with the addition of an EEG system to record cortical activities. At the start of each trial, the participants had to put their right index finger pad on the left extremity of the virtual (STIMTAC) or real surface and to maintain gaze on the dot on the screen. They were instructed to stay relaxed and to focus on the material they were touching with their finger. The participants were asked to explore the surface with back and forth lateral movements of the finger continuously during 24 s. The speed (~40 mm/s) and the amplitude (~40 mm) of the finger movements as well as the exerted normal force on the surface (i.e., ~0.5 N, Fig 2), were similar to those produced by the participants of *Experiment* 1.

Two visuo-tactile stimuli from *Experiment* 1 were tested: virtual velvet/V-moving and virtual velvet/V-static. A real velvet/V-static stimuli was also tested and served as a control condition. Given that velvet was perceived from the first back-and-forth finger movement on the velvet fabrics, providing a moving visual display would have not enhanced the sensation of velvet. However, introducing a moving visual display could have shifted the participants' attentional focus towards the shinning and darkening visual traces that is away from tactile information. This external focus could have markedly altered brain activity compared to conditions where

the attentional focus was oriented on tactile information. As the real velvet condition was used as a "control condition" for comparison with the 40 back and forth movements in the virtual velvet condition, we asked the participant to maintain their attentional focus to the rubbing movement on the surface.

For trials with the virtual velvet, this image provided either a movement-induced visual feedback (V-moving) or remained static (V-static) as in *Experiment* 1 (see *Scenarios* 1 and 2). For trials with V-moving, the visual display was refreshed at the end of the trial (i.e., it appeared as in V-static display conditions). Stationary trials (no finger movement with V-static) were also recorded during 24 s and served to analyze EEG signals (see below). For reasons of homogeneity, the same auditory cues (i.e. metronome beats) as in trials with surface exploration were also delivered for the stationary trials.

For each experimental condition, the participants performed 4 trials to ensure 40 back and forth movements (i.e. Real velvet/V-static, Virtual velvet/V-static and Virtual velvet/V-moving). Four stationary trials were also recorded. The order of the condition presentation was randomized within the experiment and across participants.

Tribological measurement: Finger friction and induced vibrations

The real fabric or the STIMTAC were affixed directly on a 3 axes load cell (model 3A60-20 N, Interface Inc., Scottsdale, Arizona, recording at 2000 Hz). It provided the components of the force exerted by the finger along three orthogonal axes (the normal force F_n is along the vertical axis (perpendicular to the surface); the axes in the horizontal plane allow the calculation of the tangential force F_t). From these two forces the instantaneous coefficient of friction (COF), corresponded to F_t / F_n , is calculated. We measured both F_t and F_n and, the finger vertical acceleration while the participants were exploring the surfaces with their index finger. To measure the finger vertical vibrations induced by the friction, an accelerometer (Piezoelectric Charge Accelerometer 4374 with a charge amplifier 2635 from Bruël & Kjaer, Mennecy, France) was glued on the skin just above the nail of the right index finger. The data were acquired with Pulse software (Bruël & Kjaer, Mennecy, France). The accelerometer signal (recorded at 2000 Hz) was analyzed in the frequency domain. The variables extracted from the vibration signal are the root mean square of the acceleration (RMS) and the spectral power for 4 frequency bandwidths [3-100 Hz], [100-200 Hz], [200-400 Hz] and [400-800 Hz], following the methods and results previously described in Camillieri et al. (2018).

Brain activity (EEG)

EEG activity was recorded continuously using a Biosemi ActiveTwo system (The Netherlands, 64 Ag/AgCl electrodes, 1024 Hz sampling frequency). The EEG data were pre-processed using BrainVision Analyzer2 software (Brain Products, Gilching, Germany). EEG signals were referenced against the average of the activities recorded by all electrodes. Then, 2000 ms long epochs were extracted from the EEG signals and synchronized with respect to the point in time at which the participants started to move their index finger against the (real or simulated) velvet piles (total of 40 epochs for each participant). The onset of the movement was defined as the initial change in the tangential force towards the right (i.e., against pile). Epochs were visually inspected and those presenting artifacts were rejected. On average (across the participants), 38-40 epochs were included in the analyses.

EEG neural sources were estimated with the Dynamical Statistical Parametric Mapping (dSPM, Dale et al., 2000) implemented in the Brainstorm software (Tadel et al. 2011), which is documented and freely available for download online under the GNU general public license (http://neuroimage.usc.edu/brainstorm). A boundary element model (BEM) with three realistic layers (scalp, inner skull and outer skull) was used to compute the forward model on the anatomical MRI brain template from the Montreal Neurological Institute (MNI Colin27). Using a realistic model provides more accurate solution than a simple three concentric spheres model (Sohrabpour et al., 2015). We downsampled the cortex surface to 15 002 vertices which allowed good spatial resolution. Measuring and modelling the noise contaminating the data is beneficial to source estimation. Noise covariance matrices were computed using the stationary trials (i.e. while the participants remained still). Such EEG source reconstruction has proved to be suited for investigating the activity (which is indexed to current amplitude, Tadel et al., 2011) of outer and inner cortical surfaces with 64 sensors (Ponz et al., 2014). The current maps were averaged over 4 time-windows of 500 ms from the start of the shear forces in the against pile main direction to the end of the along pile movement direction for each participant, surfaces and visual conditions. Note that due to the metronome beats participants were accurate in completing each one-way rubbing movement in 1000 ms.

Time frequency analyses were performed in EEG source space. The data were transformed into time-frequency domain using Morlet wavelet transforms. The respective power of theta (5-7 Hz) and alpha (8-12 Hz) cortical oscillations were computed for each trial and then averaged

across trials for each condition and participant. We normalized the frequency powers by computing averaged theta and alpha event-related synchronization / desynchronization (ERS/ERD, 2000 ms epochs taken for the static trials). These computations were performed in regions of interest (ROIs) from the angular gyri of the right and left posterior parietal cortices (PPC, Brodmann area 39). These ROIs were manually defined, based on the Destrieux cortical atlas (Destrieux et al., 2010), and had both 242 vertices. We purposely selected two time windows, one from 500 to 1000 ms and one from 1000 to 1500 ms to compare changes in brain electrocortical activities (ERS/ERD) between movements against (500 to 1000 ms) and along (1000 to 1500 ms) the main pile direction. These two time windows allowed the removal of any edge effects as wavelet coefficients are less accurate at the beginning (here 0 ms) and end (here 2000 ms) of a time series (Torrence and Compo, 1998).

3.2. Statistical analyses

The analyses of the finger coefficient of friction and FIV were performed with the XLSTAT software. The objective was to compare, for each variable, two sets of data (e.g., Real velvet/V-static vs Virtual velvet/V-static) to determine if they belonged to the same population or not. In all cases, the data from the two sets were obtained from the same participants (paired data). Firstly, we verified whether each set of data followed the normal law with the Shapiro-Wilk test (p-value > 0.05). If the sets followed the normal law, the variances were compared with the Fisher-Snedecor test (F-test). In all cases for which the variances were not significantly different, the means were compared with the Student's t-test for paired data. If one or both of the two sets did not verify the normal law, the Wilcoxon signed rank test for paired data was used.

One-way ANOVAs were used to assess the effect of Condition (i.e., Real velvet/V-static, Virtual velvet with either V-static or V-moving) on the normal force, and on the theta and alpha band powers (separate analyses for the left and right inferior PPC). The time frequency analyses were performed separately for the left and right inferior PPC. For these analyses, the theta and alpha band mean powers, significant effects (statistical threshold of $p < 0.05$) were further analyzed using Newman-Keuls post-hoc tests. All data had normal distributions (as confirmed by Kolmogorov-Smirnov tests). We used t-tests ($p < 0.05$, FDR correction for multiple comparisons) to contrast the cortical current maps computed when the participants explored the

real velvet and when they explored the virtual velvet (in either the V-static or V-moving visual display).

3.3. Results

Tribological results

The participants complied with the requirement to exert a ~0.5 N normal force with the index finger during the surface exploration (overall mean of 0.51 N ± 0.15, Fig. 2). The ANOVA showed that this force did not significantly differ between the different visual and tactile conditions ($F_{2,26} = 2.30$; $p = 0.11$).

Figure 3 shows substantial variation in the CoF among participants. The closer a point is to the dotted line, the better the correspondence between the tested surfaces. The high correlation (R^2=0.96) between virtual velvet with V-static and V-moving is not surprising since the same smooth surface (STIMTAC) was tested with the same tactile stimulus. Although Figure 3B highlights a good correspondence between real and virtual fabrics (R^2=0.72), most participants demonstrated a higher CoF when moving on virtual velvet compared to real velvet fabric. However, for 4 participants, the opposite trend was observed. When comparing the 4 participants who exhibited this tendency with the 3 participants with the highest CoF for the virtual velvet, we found that the gender of the participants was not an issue. Rather, skin hydration levels appear as a relevant factor. Participants with lower CoF values showed lower skin hydration (mean of 55 a.u., less hydration), while those with high CoF values had higher skin hydration (i.e., 83 a.u.). This finding is consistent with previous research indicating that the CoF between the finger and a surface depends on the hydrolipid film composition, specifically the water-to-lipid ratio, especially when interacting with a smooth surface as STIMTAC (Cornuault et al., 2015).

Figure 4 shows the FIV (i.e. the RMS of the finger vertical acceleration) for the 3 surface/visual display conditions (Fig 4A-C). The averaged FIV autospectra had the same global shape between conditions. However, across the FIV frequencies, the RMS distribution was smaller when the participants explored the real velvet compared to the virtual velvet. Moreover, in conditions with a V-static display, exploring the virtual surface yielded greater RMS than when exploring a real velvet with static display (Fig. 4D). For the virtual velvet, the autospectra was very similar between both visual stimuli (i.e., V-static and V-moving, Fig. 4E).

The box plots of the spectral power (Fig. 5) confirmed that the variability between the participants was lower with the real velvet, whatever the frequency bandwidth. Moreover, the

p-values for the spectral powers obtained for the different bandwidths show that the FIV when rubbing the real velvet and the virtual velvet with V-static were significantly different between 100 and 400 Hz (ps < 0.05, Fig. 5B-C). As expected, there was no significant difference on the FIV between the V-moving or V-static conditions with the virtual velvet (p>0.05, Fig. 5A-D).

Brain activity

Surface-specific source localization

Figure 6 shows the statistical cortical maps for two different contrasts. As a striking result, the topography of the cortical activations estimated by source analyses differed greatly between the V-moving and V-static (compare Fig. 6A and Fig. 6B). The effect of the visual display was particularly noticeable when contrasting the real with the virtual velvet with V-moving (attested by the cold/blue colors of the cortical regions in Fig. 6A). Indeed, during virtual velvet finger exploration, the lateral occipital (LOC) and inferior PPC, and the medial surface of the left PPC (precuneus) of the right hemisphere showed significantly greater activation in the contrast Real velvet/V-Static minus Virtual velvet/V-moving conditions but not in the contrast Real velvet/V-Static minus Virtual velvet/V-static. The greater activity of the PPC observed with the Virtual surface persisted throughout the exploring finger movements, except for the left precuneus whose activity was significantly greater only at the beginning of the movement against pile main direction [0-500 ms]. Note that in both contrasts (Fig. 6A-B), the right dorsal anterior cingulate cortex (ACC) showed greater activation when moving on the virtual surface solely at the beginning of the movement against pile [0-500 ms] regardless of the visual feedback.

Moreover, moving the finger on a real velvet fabric engaged greater activity of the left motor area (i.e., contralateral to the moving finger) than when moving on a virtual velvet (i.e. warm/red colors in pre-rolandic cortex, Fig. 5). Interestingly, this enhanced motor activity was observed when the participants moved their index finger both against and along the pile in the V-moving condition, but only when the finger moved against the pile in the V-static display condition. The increased activation of the left sensorimotor region with real velvet was accompanied with a greater activity of the right PPC BA 40 (rostral to BA 39), that was only observed when participants received V-moving feedback during their movement.

Modulation of theta (5-7 Hz) oscillations in the left inferior PPC

Time-frequency analyses performed on the left and right PPC ROI (Fig. 7A) showed that theta band power was significantly impacted by the conditions (surface/visual feedback). This effect was observed for the left PPC when the participants moved their index finger along the pile ($F_{2,24} = 5.55$; $p = 0.01$, Fig. 7B, right panel). Post-hoc analyses revealed that the mean theta power was greater in the Virtual velvet/V-moving condition than in both the Real velvet/V-static ($p = 0.013$) and Virtual velvet/V-static ($p = 0.015$) conditions. Note that a significant desynchronization (ERD) was observed for both conditions with a V-static visual display (t-test for means against a value 0; $t_{12} = -3.36$, $p = 0.0055$ and $t_{12} = -3.59$; $p = 0.0036$, respectively for the Real velvet and Virtual velvet). No significant effect of condition was observed on theta band power for the movements against pile (Fig. 7B, left panel $F_{2,24} = 2.79$; $p = 0.08$) or for the right PPC ($F_{2,24} = 1.04$; $p = 0.36$ and $F_{2,24} = 1.47$; $p = 0.24$ for the along pile and against pile movement, respectively). The effect of condition on the alpha band power computed in the left and right PPC ROIs was not significantly different ($ps > 0.05$).

4. Discussion

We investigated the perceptual rendering of virtual velvet fabric from tactile simulation (*Experiment 1*) together with the behavioral and neurophysiological substrates subserving this perception (*Experiment 2*). Our core objective was to test the possibility of improving velvet fabric rendering of a tactile device by adding the visual effects of rubbing a velvet fabric with a finger. The originality of our study lies in the fact that the participants could not see their moving finger (vision of the hand was occluded), but only a visual simulation of the trails left on a velvet fabric Specifically, when the participants moved their index finger against or along the main direction of the pile simulated by the tactile device, the visual display left a darker and lighter trace, respectively.

In a previous experiment, it was shown that the STIMTAC device used in the present study failed to simulate real velvet fabric (Camillieri et al., 2018). Our results suggest this could be due, in part, from the COF and the RMS of the vertical finger acceleration which differed when our participants explored the virtual velvet and the real velvet (*Experiment* 2). Remarkably, however, when the same tactile stimulation was combined with the visual rendering of a real velvet being rubbed by the participant's finger, the surface of the explored tactile device was perceived as being rougher (*Experiment* 1). Because the attribute "rough" is a predominant velvet descriptor (Bassereau and Charvet-Pellot, 2011), this result could be construed as

evidence that the dynamic velvet-like visual simulation enhanced the tactile-induced velvet perception. This enhancement may be due to the increase in roughness related to the against the grain movement.

Our perceptive and behavioral results then point to a crossmodal integration between tactile and visual information that can alter the touch sensation. Note, however, that the "velvet effect" (i.e., descriptor chosen to describe the effect of the pile tuft under the fingers) was not observed when the dynamic velvet image (V-moving) was combined with a tactile stimulus that did not relate to any known fabrics (i.e., sham stimulation in *Experiment* 1). This might suggest a near-effective skin/surface interaction in the present T_{Vel} condition for enabling a velvet rendering. This hypothesis is supported by studies showing that near sensory threshold stimulations can be perceived if combined with coherent stimulation from other sensory modalities (e.g., Popov et al., 1999; Dalton et al., 2000). It is also in line with those studies showing a more efficient integration of visual feedback in conditions with degraded somatosensory inputs (e.g., Mizelle et al., 2016; Tsay et al., 2021, see Limanowski, 2022 for a review).

The increased activity observed in the occipital and inferior parietal lobes (*Experiment 2*) could underlie the crossmodal sensory processes when velvet-like movement-induced visual feedback and tactile stimulus were combined. This would be consistent with the fMRI study of Limanowski and Blankenburg (2017) showing that these two posterior cortical regions work together to evaluate visuo-tactile congruence between the seen and the felt (tactile) hand positions. Increasing the congruence between visual and tactile cues during the active finger movements may have prompted the binding effect that denotes the mutual attraction between the visual perception of the velvet pile bending under the caressing finger and the simulated tactile inputs generated by the sliding finger on the tactile device.

In the left PPC, the power of theta band oscillations was markedly greater in the condition combining velvet-like tactile stimulation and movement-induced visual feedback than in both conditions with a static visual display (with either real or virtual velvet tactile stimulation). Interestingly, in the former condition, the participants of *Experiment 1* perceived the explored surface as being rougher than in both conditions with a static visual display, which used velvet-like or sham tactile stimulations). Previous studies showed evidence that increases in theta power enhance visuo-tactile integration processes (see Kanayama & Ohira 2009). In the present study, the greater theta power was observed over the left PPC, i.e. in the hemisphere contralateral to the moving finger, when the participants' index finger was moving along the pile. Because integrative processes take ~250 ms (see Kanayama & Ohira 2009), the fact that

the increased theta power was observed from the very beginning of the finger movement along the pile direction suggests that this change of theta power started during the against pile /along pile reverse movement. Theta oscillations could be instrumental in binding visuo-tactile information to increase touch sensation. This is supported by studies showing that higher amplitudes of theta oscillations encode for touch intensity (Michail et al., 2016), fabric physical properties (e.g., warmness, softness, overall comfort, Jiao et al., 2020) as well as for more salient sensory stimuli (Iannetti et al., 2008). The dynamic velvet-like visual feedback could have also primed tactile representation of the velvet fabric. Such priming effect is consistent with the Brunyé et al.'s (2012) discovery that reading about tactile properties affects the subsequent tactile perception. More specifically, the authors found that all fabric ratings became smoother after reading a sentence implying a smooth tactile property, and rougher after reading a sentence implying a rough tactile property. In *Experiment* 1, the participants perceived the virtual tactile surface as being roughest in the condition that combined the velvet-like tactile, i.e. T_{Vel}, and dynamic visual stimulations. Combining either movement-induced visual feedback with sham tactile stimulation or velvet-like tactile stimulation with a static image of a velvet fabric decreased the roughness perception of the explored surface. Together, these findings suggest that visuo-tactile sensory integration and sensory priming effect are not the most critical aspects for perceiving a tactile device as being rough. Rather, the relatedness between tactile and visual feedback clearly emerged in the present study as the most relevant factor.

The greater activations of the right occipital and lateral occipital cortices and of the inferior PPC (BA 39) were found in the condition with velvet-like dynamic tactile and visual stimulations compared to the condition with real velvet and a static image of a velvet fabric. This increased activity, which was observed throughout the finger exploration of the tactile device (i.e., no effect of movement direction with respect to the simulated main pile direction), could have contributed to the emergence of a velvet representation with simulation of velvet-related tactile and visual information. More specifically, the greater occipital activity could be linked to the observation made by Stilla and Sathian (2008) that visual and haptic texture-selectivity overlaps in the right occipital cortex. These authors found evidence for this bimodal texture-related selectivity in a fMRI study after contrasting shape-related selectivity and visual and haptic texture-selectivity. The LOC, which also showed greater activity in the condition with velvet-like dynamic tactile and visual stimulations, is known to be responsive to visual and tactile inputs (Amedi et al., 2001; Stilla and Sathian, 2008). However, there is clear evidence that the role of the LOC goes beyond the mere stimuli recognition, and that this

functional region is part of a network involved in object representation and recognition. For instance, Kim and Zatorre (2011) showed that the LOC is commonly active during shape discrimination through different sensory modalities (visual, tactile, and auditory). Based on this finding and on the fact that the middle longitudinal fasciculus (i.e. main long-range fiber bundle) courses from the LOC through the inferior parietal lobule (Palejwala et al., 2020), we suggest that providing a visual rendering of a virtual surface explored by a finger may have prompted the velvet-like representation and perception.

Acknowledgments

We thank Professor Betty Lemaire-Semail, from L2EP/IRCICA (University of Lille), for making available the STIMTAC tactile simulator with the support of the GDR TACT (CNRS 2033).

Funding

This work was supported by the project COMTACT (ANR 2020-CE28-0010-03), funded by the french "Agence Nationale de la Recherche" (ANR).

Data accessibility

The data are made available from the Zenodo repository DOI: 10.5281/zenodo.13710303 or https://zenodo.org/records/13710303

References

Amedi, A., Malach, R., Hendler, T., Peled, S., & Zohary, E. (2001). Visuo-haptic object-related activation in the ventral visual pathway. Nature neuroscience, 4(3), 324-330.

Bassereau, J.-F., & Charvet-Pello, R. (2011). Dictionnaire des mots du sensoriel. Editions Tec & Doc Lavoisier.

Baumgartner, E., Wiebel, C. B., & Gegenfurtner, K. R. (2013). Visual and haptic representations of material properties. Multisensory research, 26(5), 429-455.

Ben Messaoud, W., Bueno, M.-A., Lemaire-Semail, B. (2016). Relation between human perceived friction and finger friction characteristics. Tribology International, 98, 261‑269.

Biet, M., Giraud, F., & Lemaire-Semail, B. (2008). Implementation of tactile feedback by modifying the perceived friction. The European Physical Journal-Applied Physics, 43(1), 123-135.

Box, G. E., & Tiao, G. C. (2011). Bayesian inference in statistical analysis. John Wiley & Sons.

Breugnot, C., Bueno, M.-A., Renner, M., Ribot-Ciscar, E., Aimonetti, J.-M., Roll, J.-P. (2006). Mechanical Discrimination of Hairy Fabrics from Neurosensorial Criteria. Textile Research Journal, 76(11), 835‑846.

Brunyé, T. T., Walters, E. K., Ditman, T., Gagnon, S. A., Mahoney, C. R., Taylor, H. A. (2012). The Fabric of Thought : Priming Tactile Properties During Reading Influences Direct Tactile Perception. Cognitive Science, 36(8), 1449‑1467.

Bueno M.-A., Lemaire-Semail B., Amberg M., Giraud F. (2014). A simulation from a tactile device to render the touch of textile fabrics: a preliminary study on velvet. Textile Research Journal, 84, 1428-1440.

Bueno, M.-A., Lemaire-Semail, B., Amberg, M., Giraud, F. (2015). Pile Surface Tactile Simulation : Role of the Slider Shape, Texture Close to Fingerprints, and the Joint Stiffness. Tribology Letters, 59(1), 25.

Busch, N. A., Dubois, J., VanRullen, R. (2009). The Phase of Ongoing EEG Oscillations Predicts Visual Perception. Journal of Neuroscience, 29(24), 7869‑7876.

Busch, N. A., VanRullen, R. (2010). Spontaneous EEG oscillations reveal periodic sampling of visual attention. Proceedings of the National Academy of Sciences, 107(37), 16048‑16053.

Camillieri, B., Bueno, M.-A., Fabre, M., Juan, B., Lemaire-Semail, B., Mouchnino, L. (2018). From finger friction and induced vibrations to brain activation : Tactile comparison between real and virtual textile fabrics. Tribology International, 126, 283‑296.

Cornuault, P. H., Carpentier, L., Bueno, M. A., Cote, J. M., & Monteil, G. (2015). Influence of physico-chemical, mechanical and morphological fingerpad properties on the frictional distinction of sticky/slippery surfaces. *Journal of The Royal Society Interface*, *12*(110), 20150495.

Dale, A. M., Liu, A. K., Fischl, B. R., Buckner, R. L., Belliveau, J. W., Lewine, J. D., Halgren, E. (2000). Dynamic Statistical Parametric Mapping : Combining fMRI and MEG for High-Resolution Imaging of Cortical Activity. Neuron, 26(1).

Dalton, P., Doolittle, N., Nagata, H., & Breslin, P. A. S. (2000). The merging of the senses: integration of subthreshold taste and smell. Nature neuroscience, 3(5), 431-432.

Day, R.L. (1969). Position bias in paired product tests. Journal of Marketing Research, 6(1), 98-100.

Destrieux, C., Fischl, B., Dale, A., Halgren, E. (2010). Automatic parcellation of human cortical gyri and sulci using standard anatomical nomenclature. NeuroImage, 53(1), 1‑15.

Dionne, J. K., Meehan, S. K., Legon, W., & Staines, W. R. (2010). Crossmodal influences in somatosensory cortex: interaction of vision and touch. Human brain mapping, 31(1), 14-25.

Dione, M., Watkins, R. H., Vezzoli, E., Lemaire-Semail, B., Wessberg, J. (2021). Human low-threshold mechanoafferent responses to pure changes in friction controlled using an ultrasonic haptic device. Scientific Reports, 11(1), 11227.

Driver, J., Spencer, C. (2000). Multisensory perception : Beyond modularity and convergence. Current Biology, 10(20), 731‑735.

Ernst, M. O., & Banks, M. S. (2002). Humans integrate visual and haptic information in a statistically optimal fashion. *Nature*, *415*(6870), 429-433.

Fabre, M., Beullier, L., Sutter, C., Kebritchi, A., Chavet, P., Simoneau, M., Mouchnino, L. (2023). Cortical facilitation of somatosensory inputs using gravity-related tactile information in humans with vestibular hypofunction. Journal of Neurophysiology, 130(1), 155-167.

Faucheu, J., Weiland, B., Juganaru-Mathieu, M., Witt, A., Cornuault, P.-H. (2019). Tactile aesthetics : Textures that we like or hate to touch. Acta Psychologica, 201, 102950.

Felicetti, L., Chatelet, E., Latour, A., Cornuault, P. H., Massi, F. (2022). Tactile rendering of textures by an electro-active polymer piezoelectric device: mimicking friction-induced vibrations. Biotribology, 31, 100211.

Giboreau, A., Navarro, S., Faye, P., Dumortier, J. (2001). Sensory Evaluation of Automotive Fabrics: The Contribution of Categorization Tasks and Non Verbal Information to Set-up a Descriptive Method of Tactile Properties. Food Quality and Preference, 12(5–7).

Grigorii, R. V., Peshkin, M. A., Colgate, J. E. (2019). Stiction rendering in touch. In 2019 IEEE World Haptics Conference (WHC) (pp. 13-18). IEEE.

Haegens, S., Händel, B. F., Jensen, O. (2011). Top-Down Controlled Alpha Band Activity in Somatosensory Areas Determines Behavioral Performance in a Discrimination Task. The Journal of Neuroscience, 31(14), 5197‑5204.

Hage, J. J., Van der Steen, L. P. E., de Groot, P. J. M. (1995). Difference in sensibility between the dominant and nondominant index finger as tested using the Semmes-Weinstein monofilaments pressure aesthesiometer. The Journal of Hand Surgery, 20A, 227‑229.

Harrington, T., Merzenich, M. M. (1970). Neural coding in the sense of touch: Human sensations of skin indentation compared with the responses of slowly adapting mechanoreceptive afferents innervating the hairy skin of monkeys. Experimental Brain Research, 10(3), 251-264.

Hidaka, S., Teramoto, W., Sugita, Y. (2015). Spatiotemporal processing in crossmodal interactions for perception of the external world: a review. Frontiers in integrative neuroscience, 9, 62.

Ho, Y.-X., Landy, M. S., Maloney, L. T. (2006). How direction of illumination affects visually perceived surface roughness. Journal of Vision, 6(5), 8.

Iannetti, G. D., Hughes, N. P., Lee, M. C., Mouraux, A. (2008). Determinants of Laser-Evoked EEG Responses: Pain Perception or Stimulus Saliency? Journal of Neurophysiology, 100(2), 815‑828.

Ishida, H., Nakajima, K., Inase, M., & Murata, A. (2010). Shared mapping of own and others' bodies in visuotactile bimodal area of monkey parietal cortex. Journal of Cognitive Neuroscience, 22(1), 83-96.

Jiao, J., Hu, X., Huang, Y., Hu, J., Hsing, C., Lai, Z., Wong, C., Xin, John. H. (2020). Neuro-perceptive discrimination on fabric tactile stimulation by electroencephalographic (EEG) spectra. PLOS ONE, 15(10), 1‑15.

Johansson, R. S., Vallbo, Å. B. (1983). Tactile sensory coding in the glabrous skin of the human hand. Trends in neurosciences, 6, 27-32.

Kanayama, N., and Ohira, H. (2009). Multisensory processing and neural oscillatory responses : Separation of visuotactile congruency effect and corresponding electroencephalogram activities. NeuroReport, 20(3), 289‑293.

Kim, J.-K., Zatorre, R. J. (2011). Tactile–Auditory Shape Learning Engages the Lateral Occipital Complex. The Journal of Neuroscience, 31(21), 7848‑7856.

Klatzky, R., Lederman, S. J. Reed, C. (1989). Haptic integration of object properties: texture, hardness and planar contour. Journal of Experimental Psychology: Human Perception and Performance, 15(1), 45-57.

Kruschke, J. K. (2010). What to believe: Bayesian methods for data analysis, Trends in Cognitive Sciences 14, 293–300.

Liesner, M., Kunde, W. (2020). Suppression of mutually incompatible proprioceptive and visual action effects in tool use. PlosOne, 15(11), e0242327.

Limanowski, J. (2022). Precision control for a flexible body representation. Neuroscience and Biobehavioral Reviews, 134, 104401.

Limanowski, J., Blankenburg, F. (2017). Posterior parietal cortex evaluates visuoproprioceptive congruence based on brief visual information. Scientific Reports, 7(1), 16659.

Manfredi, L. R., Saal, H. P., Brown, K. J., Zielinski, M. C., Dammann III, J. F., Polashock, V. S., Bensmaia, S. J. (2014). Natural scenes in tactile texture. Journal of neurophysiology, 111(9), 1792-1802.

Massimiani, V., Benjamin, W., Eric, C., Pierre-Henri, C., Jenny, F., Francesco, M. (2020). The role of mechanical stimuli on hedonistic and topographical discrimination of textures. Tribology International, 143, 106082.

Michail, G., Dresel, C., Witkovský, V., Stankewitz, A., Schulz, E. (2016). Neuronal Oscillations in Various Frequency Bands Differ between Pain and Touch. Frontiers in Human Neuroscience, 10.

Mizelle, J. C., Oparah, A., Wheaton, L. A. (2016). Reliability of visual and somatosensory feedback in skilled movement: the role of the cerebellum. Brain topography, 29, 27-41.

Palejwala, A. H., O'Connor, K. P., Pelargos, P., Briggs, R. G., Milton, C. K., Conner, A. K., Milligan, T. M., O'Donoghue, D. L., Glenn, C. A., Sughrue, M. E. (2020). Anatomy and white matter connections of the lateral occipital cortex. Surgical and Radiologic Anatomy, 42(3), 315‑328.

Penny J.C., Hunt I.M. Twyman W.A. (1972). Product testing methodology in relation to marketing problems. Journal of the Marketing Research Society, 14.

Pfurtscheller, G., Lopes da Silva, F. H. (1999). Event-related EEG/MEG synchronization and desynchronization : Basic principles. Clinical Neurophysiology, 110(11).

Ponz, A., Montant, M., Liegeois-Chauvel, C., Silva, C., Braun, M., Jacobs, A. M., Ziegler, J. C. (2014). Emotion processing in words : A test of the neural re-use hypothesis using surface and intracranial EEG. Social Cognitive and Affective Neuroscience, 9(5), 619‑627.

Popov, K. E., Kozhina, G. V., Smetanin, B. N., Shlikov, V. Y. (1999). Postural responses to combined vestibular and hip proprioceptive stimulation in man. European Journal of Neuroscience, 11(9), 3307-3311.

Romo, R., Hernández, A., Zainos, A., & Salinas, E. (2003). Correlated neuronal discharges that increase coding efficiency during perceptual discrimination. Neuron, 38(4), 649-657.

Sereno, M. I., and Huang, R.-S. (2014). Multisensory maps in parietal cortex. Current Opinion in Neurobiology, 24, 39‑46.

Sohrabpour, A., Yunfeng, L., Bin, H. (2015). Estimating underlying neuronal activity from EEG using an iterative sparse technique. Annual International Conference of the IEEE Engineering in Medicine and Biology Society, 634‑637.

Stilla, R., Sathian, K. (2008). Selective visuo-haptic processing of shape and texture. Human Brain Mapping, 29(10), 1123‑1138.

Tadel, F., Baillet, S., Mosher, J. C., Pantazis, D., Leahy, R. M. (2011). Brainstorm: A User-Friendly Application for MEG/EEG Analysis. Computational Intelligence and Neuroscience, 2011, 1‑13.

Tiest, W. M. B., Kappers, A. M. (2007). Haptic and visual perception of roughness. Acta psychologica, 124(2), 177-189.

Torrence, C., Compo, G. P. (1998). A practical guide to wavelet analysis. Bulletin of the American Meteorological Society, 79(1), 61-78.

Tsay, J. S., Avraham, G., Kim, H. E., Parvin, D. E., Wang, Z., Ivry, R. B. (2021). The effect of visual uncertainty on implicit motor adaptation. Journal of Neurophysiology, 125(1), 12‑22.

Weiland B, Leclinche F, Kaci A, Camillieri B, Lemaire-Semail B, Bueno M-A. (2024) Tactile simulation of textile fabrics: Design of simulation signals with regard to fingerprint. Tribol Int. 191:109113.

Wulf G & Prinz W (2001) Directing attention to movement effects enhances learning : A review. Psychonomic Bulletin & Review, 8(4), 648-660.

Zhou, Y. D., Fuster, J. M. (2000). Visuo-tactile cross-modal associations in cortical somatosensory cells. Proceedings of the National Academy of Sciences, 97(17), 9777-9782.

Figure caption

Figure 1: Experimental set up. The tactile stimulator STIMTAC is fixed on a three axes load cell. The screen in front of the participants shows either a static visual display (V-static) or a movement-induced visual feedback (V-moving). The right index finger is equipped with the accelerometer for the experiment 2.

Figure 2: Mean normal force for all participants (N = 14). Error bars represent standard deviation across participants.

Figure 3: Coefficients of friction for all the participants: **A)** for virtual and real velvet fabrics (the dashed line is the line y = x), **B)** for the virtual velvet for V-static and V-moving visual feedback. A dot corresponds to a participant.

Figure 4: Acceleration autospectra obtained for all the participants. The average autospectrum is in black and the standard deviation in grey. **A)** for the real velvet with V-static visual display, **B**) for the virtual velvet with V-static and **C**) for the virtual velvet with V-moving. **D**) Average acceleration autospectra for all the participants obtained for the real and virtual velvet with V-static visual display, **E**) for the virtual velvet with V-static or V-moving.

Figure 5: Box plot for the spectral power of acceleration for all the participants obtained for the real velvet with V-static, for virtual velvet with V-static and V-moving for different bandwidths: **A**) 3 to 100 Hz, **B**) 100 to 200 Hz, **C)** 200 to 400 Hz and **D**) 400 to 800 Hz. The middle line in the box plot is the median and the red cross the mean.

Figure 6: Statistical source estimation maps for real velvet versus virtual velvet fabric with V-moving (**A**), and versus virtual velvet with V-static (**B**) contrasts. Significant t-values ($p \leq 0.05$, n = 14) of the source localization were shown during the 4 time window of 500 ms starting at the movement against pile main direction onset to the end of the along pile movement. Sources are projected on a cortical template (MNI's Colin 27). For the first 500 ms contrast, we display the top and the left inner cortical views. Not surprisingly, we found that, compared to the exploration of the virtual velvet, the exploration of the real velvet resulted in greater activation in frontal areas as the supplementary motor and the dorsal premotor cortices suggesting a greater tactile stimulation intensity.

Figure 7: **A**) Time-frequency power (ERS/ERD) of the signals by means of a complex Morlet's wavelet transform applied on the ROIs for each trial of each participant then averaged across participants. Cooler colors indicate ERD (event-related desynchronization) while warmer colors indicate ERS (event-related synchronization). Frequency bands of theta and alpha bands are illustrated to present changes in brain electrocortical activity. **B)** Group means power for Theta (5-7 Hz) frequency band computed during [500; 1000 ms] (left panel) and [1000; 1500 ms] (right panel) time windows (error bars depict standard error of the mean) over the left and right PPC.

Table 1 Visuo-tactile stimuli used in *Experiment 1.*

STIMTAC Tactile stimulus	**Visual feedback**	
virtual velvet	V-moving	V-static
virtual sham	V-moving	V-static

Table 2: Observed frequencies that tactile stimulus in virtual velvet/V-moving is perceived rougher than in the other visuo-tactile stimuli.

Paired comparisons	α=virtual velvet/V-static	α = virtual sham/V-moving	α =virtual sham/V-static
Observed frequency of occurrence that tactile stimulus in virtual velvet/V-moving is perceived rougher when presented in first position	**0.32**	**0.36**	**0.41**
Observed frequency of occurrence that tactile stimulus in visuo-tactile stimulus α is perceived rougher when presented in first position	0.14	0.18	0.23
Observed frequency of occurrence that tactile stimulus in virtual velvet/V-moving is perceived rougher when presented in second position	**0.55**	**0.55**	**0.68**
Observed frequency of occurrence that tactile stimulus in visuo-tactile stimulus α is perceived rougher when presented in second position	0.41	0.41	0.55

Table 3 : Scores of roughness expressed as probabilities and computed using Bayesian inference

Paired comparisons (α vs β)	α rougher than β	α equal β	β rougher than α
virtual velvel/V-moving vs virtual velvet/V-static	0.49	0.19	0.32
virtual velvel/V-moving vs virtual sham/V-moving	0.52	0.15	0.33
virtual velvel/V-moving vs virtual sham/V-static	0.56	0.04	0.40
virtual velvet/V-static vs virtual sham/V-moving	0.60	0.04	0.36
virtual velvet/V-static vs virtual sham/V-static	0.31	0.17	0.52
virtual sham/V-moving vs virtual sham/V-static	0.36	0.14	0.50

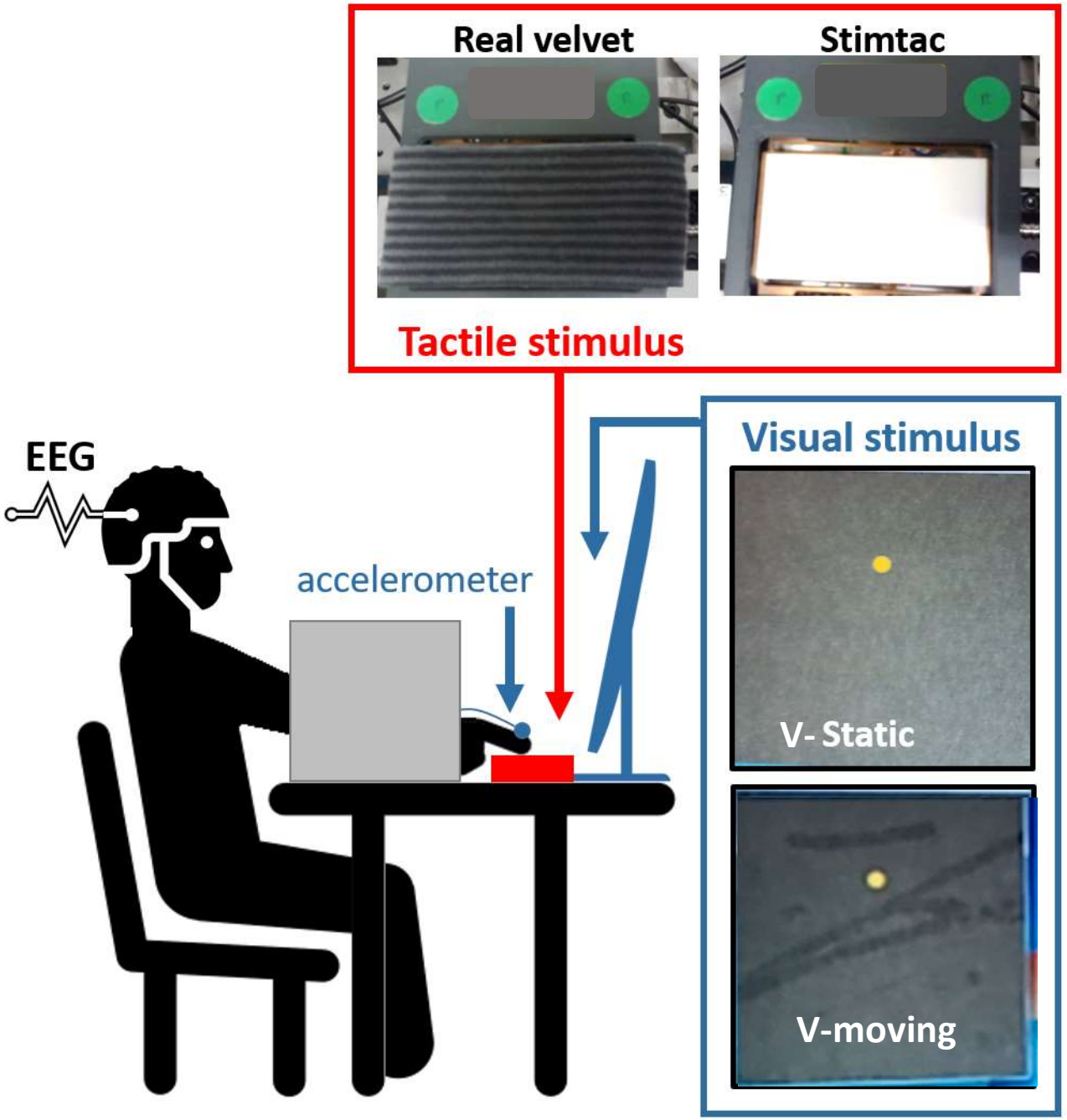
Real velvet
Stimtac
Tactile stimulus
EEG
accelerometer
Visual stimulus
V- Static
V-moving

Figure 1

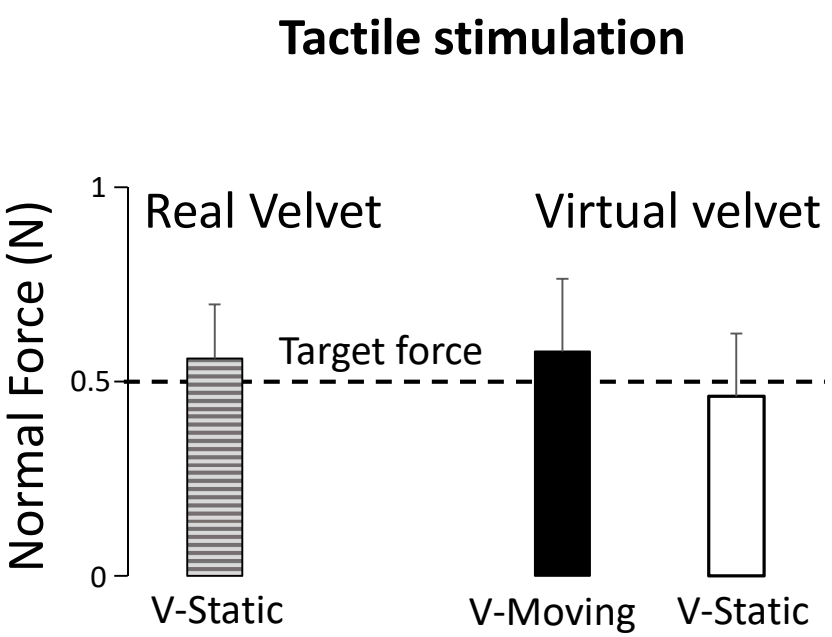
Tactile stimulation
Normal Force (N)
1
0.5
0
Real Velvet
Virtual velvet
Target force
V-Static
V-Moving
V-Static

Figure 2

Coefficient of Friction

A)

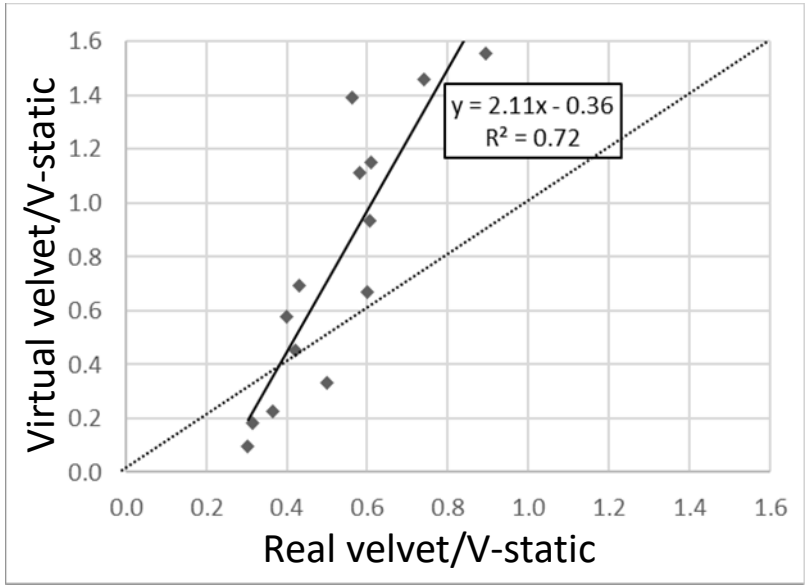

B)

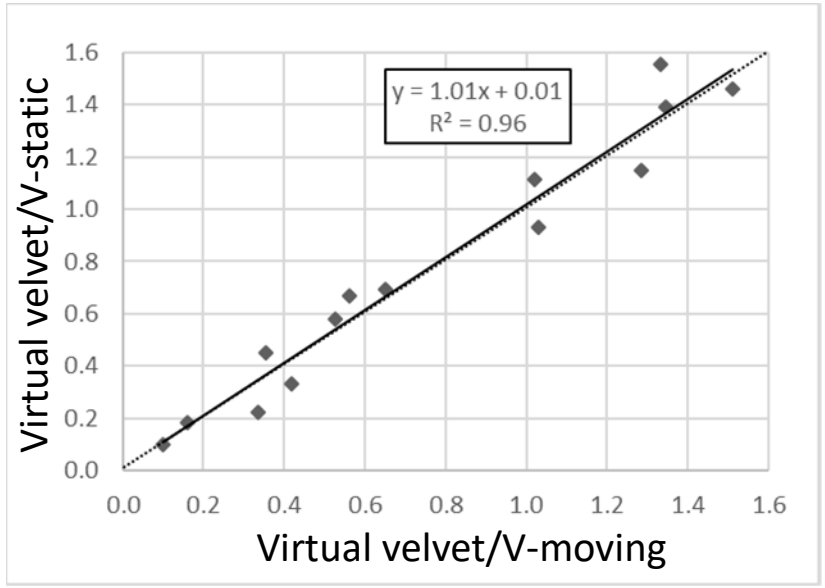

Figure 3

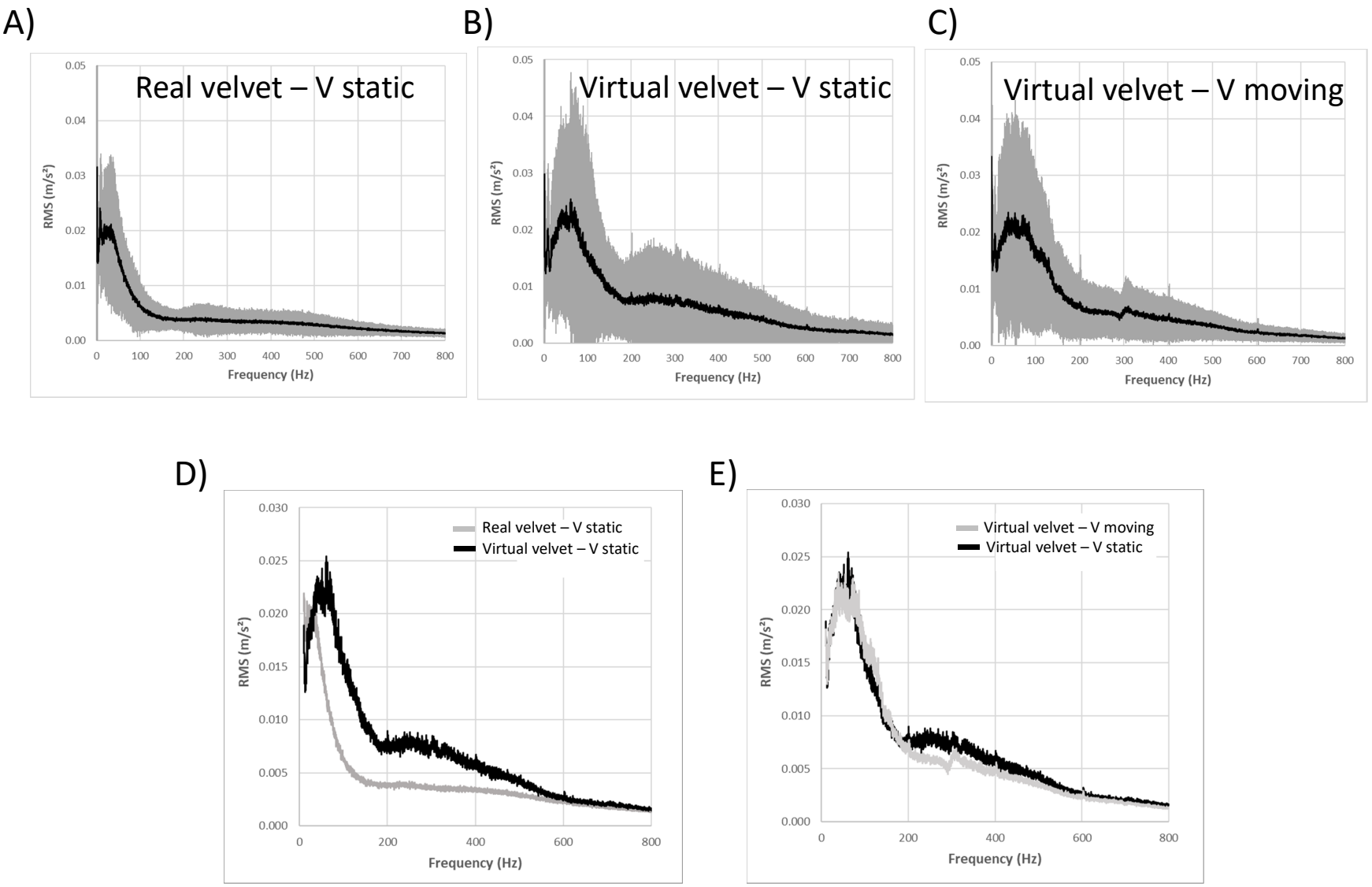
A)
Real velvet – V static
B)
Virtual velvet – V static
C)
Virtual velvet – V moving
RMS (m/s²)
Frequency (Hz)
D)
Real velvet – V static
Virtual velvet – V static
E)
Virtual velvet – V moving
Virtual velvet – V static

Figure 4

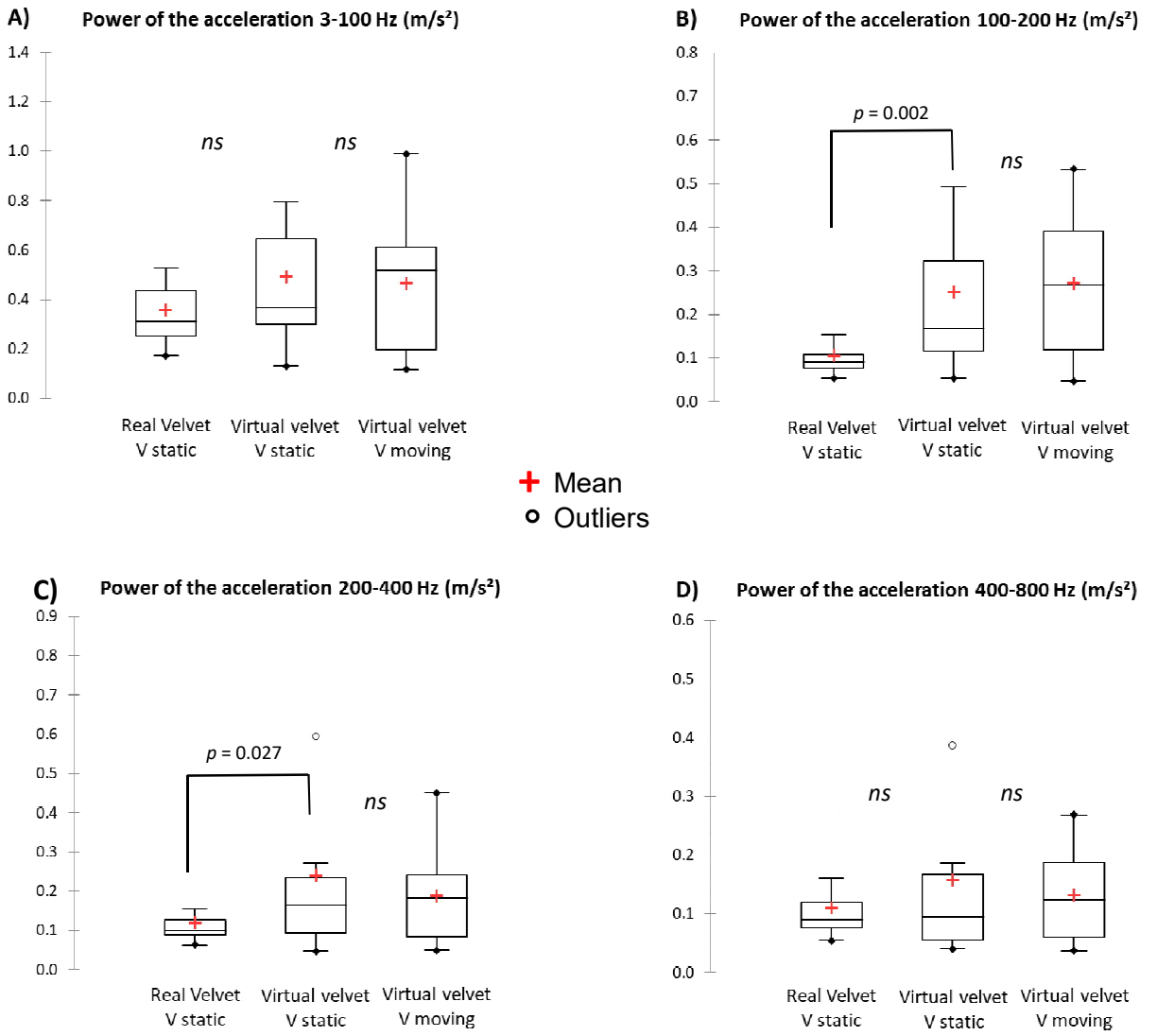
A)
Power of the acceleration 3-100 Hz (m/s²)
1.4
1.2
1.0
0.8
0.6
0.4
0.2
0.0
ns
ns
Real Velvet V static
Virtual velvet V static
Virtual velvet V moving
B)
Power of the acceleration 100-200 Hz (m/s²)
0.8
0.7
0.6
0.5
0.4
0.3
0.2
0.1
0.0
p = 0.002
ns
Real Velvet V static
Virtual velvet V static
Virtual velvet V moving
Mean
Outliers
C)
Power of the acceleration 200-400 Hz (m/s²)
0.9
0.8
0.7
0.6
0.5
0.4
0.3
0.2
0.1
0.0
p = 0.027
ns
Real Velvet V static
Virtual velvet V static
Virtual velvet V moving
D)
Power of the acceleration 400-800 Hz (m/s²)
0.6
0.5
0.4
0.3
0.2
0.1
0.0
ns
ns
Real Velvet V static
Virtual velvet V static
Virtual velvet V moving

Figure 5

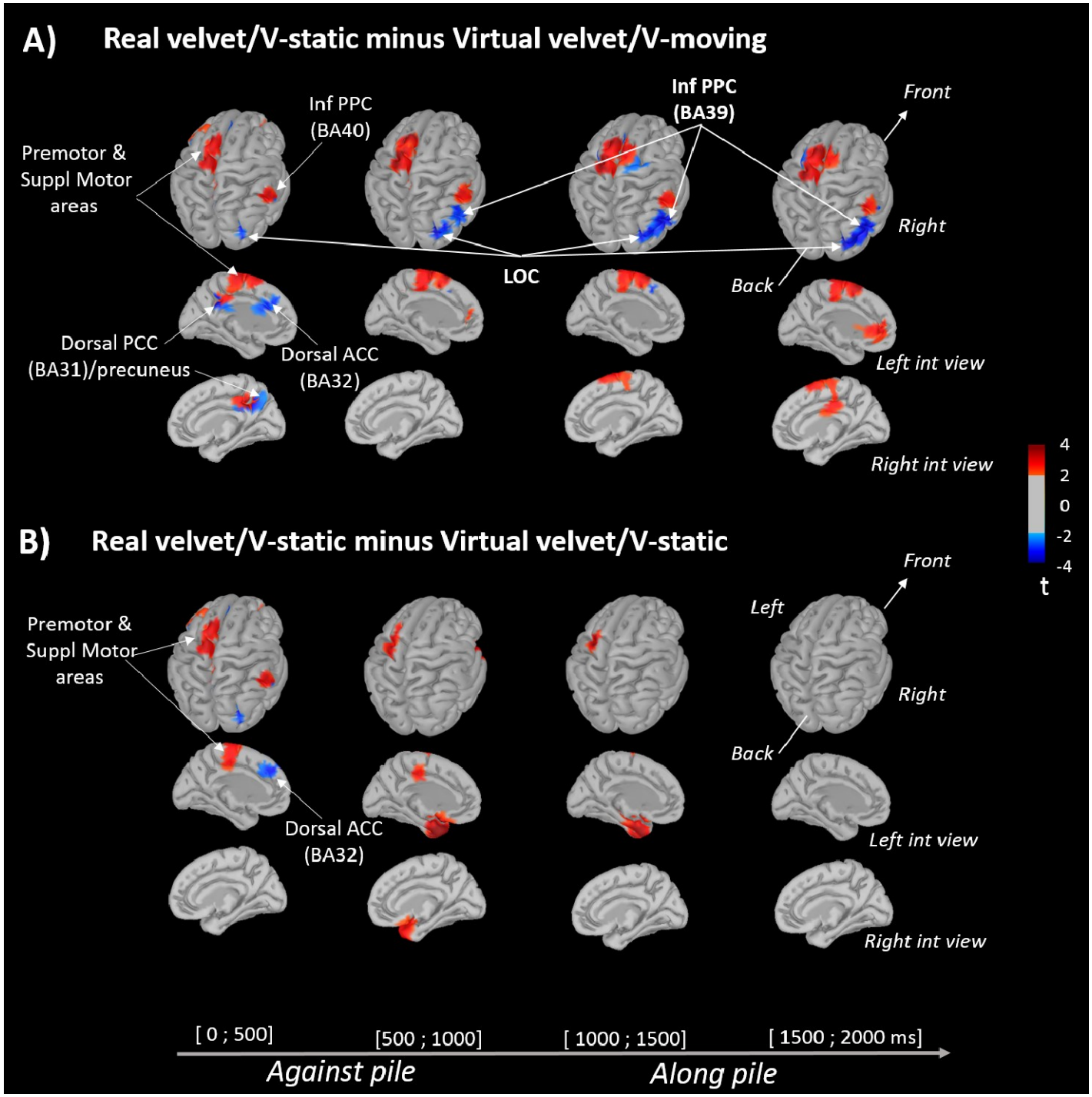
A) Real velvet/V-static minus Virtual velvet/V-moving
Inf PPC (BA40)
Inf PPC (BA39)
Front
Premotor & Suppl Motor areas
Right
LOC
Back
Dorsal PCC (BA31)/precuneus
Dorsal ACC (BA32)
Left int view
Right int view
4
2
0
-2
-4
t
B) Real velvet/V-static minus Virtual velvet/V-static
Front
Left
Premotor & Suppl Motor areas
Right
Back
Dorsal ACC (BA32)
Left int view
Right int view
[0 ; 500]
[500 ; 1000]
[1000 ; 1500]
[1500 ; 2000 ms]
Against pile
Along pile

Figure 6

A)

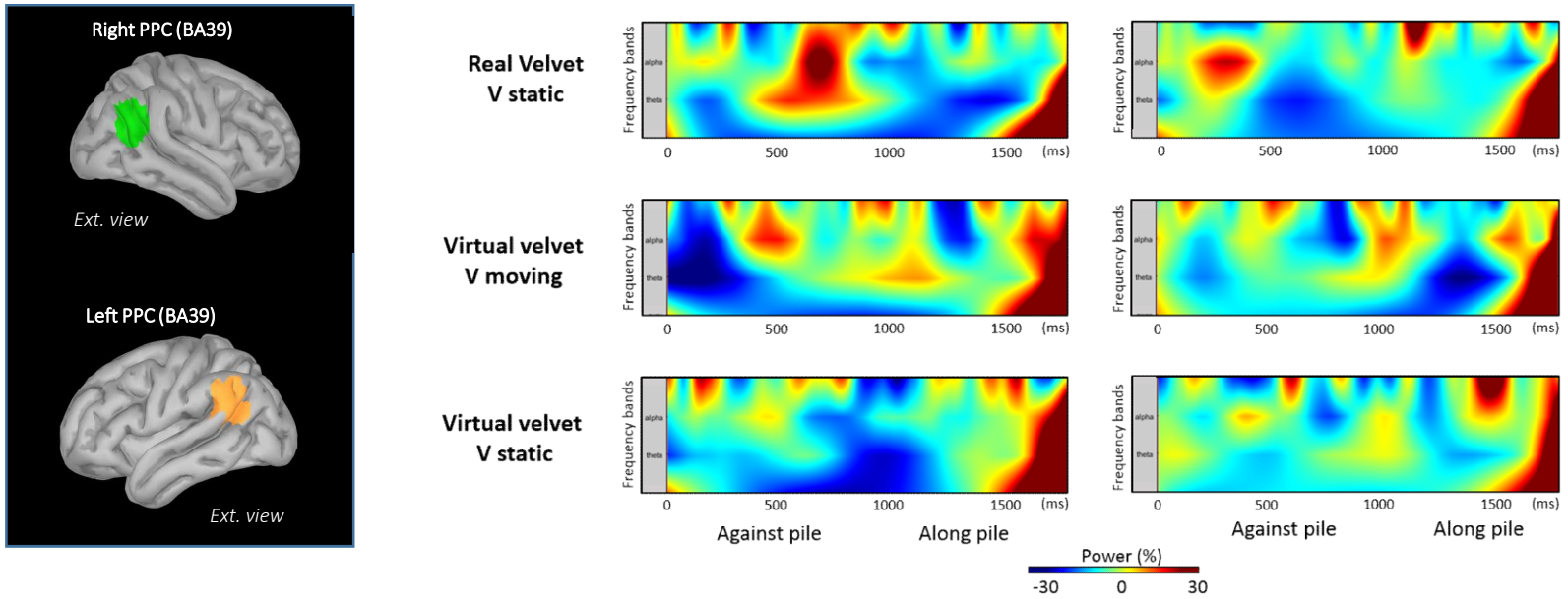
Regions of interest
Right PPC (BA39)
Ext. view
Left PPC (BA39)
Ext. view
Left PPC (BA39)
Right PPC (BA39)
Real Velvet
V static
Virtual velvet
V moving
Virtual velvet
V static
Frequency bands
alpha
theta
0
500
1000
1500
(ms)
Against pile
Along pile
Power (%)
-30
0
30

B)

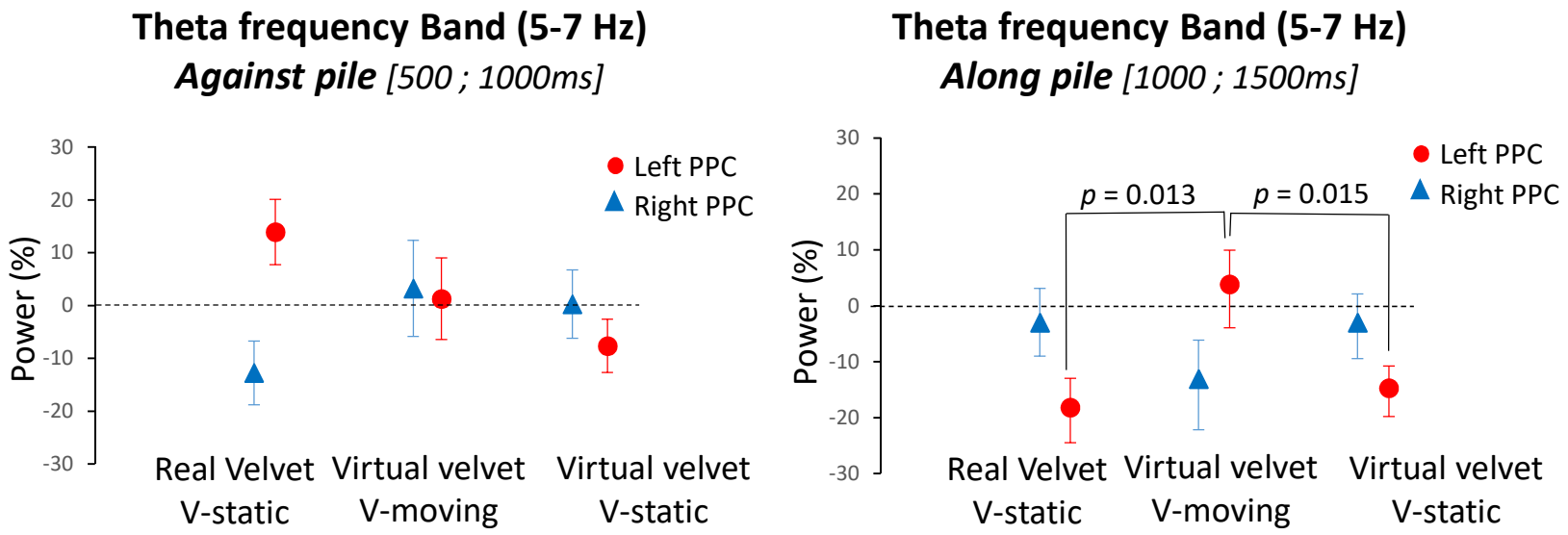
Theta frequency Band (5-7 Hz)
Against pile [500 ; 1000ms]
Theta frequency Band (5-7 Hz)
Along pile [1000 ; 1500ms]
Power (%)
30
20
10
0
-10
-20
-30
Left PPC
Right PPC
p = 0.013
p = 0.015
Real Velvet
V-static
Virtual velvet
V-moving
Virtual velvet
V-static

Figure 7

Table 1 Visuo-tactile stimuli used in *Experiment 1*.

STIMTAC Tactile stimulus	**Visual feedback**	
virtual velvet	V-moving	V-static
virtual sham	V-moving	V-static

Table 2: Observed frequencies that tactile stimulus in virtual velvet/V-moving is perceived rougher than in the other visuo-tactile stimuli.

Paired comparisons	α=virtual velvet/V-static	α = virtual sham/V-moving	α =virtual sham/V-static
Observed frequency of occurrence that tactile stimulus in virtual velvet/V-moving is perceived rougher when presented in first position	**0.32**	**0.36**	**0.41**
Observed frequency of occurrence that tactile stimulus in visuo-tactile stimulus α is perceived rougher when presented in first position	0.14	0.18	0.23
Observed frequency of occurrence that tactile stimulus in virtual velvet/V-moving is perceived rougher when presented in second position	**0.55**	**0.55**	**0.68**
Observed frequency of occurrence that tactile stimulus in visuo-tactile stimulus α is perceived rougher when presented in second position	0.41	0.41	0.55

Table 3 : Scores of roughness expressed as probabilities and computed using Bayesian inference

Paired comparisons (α vs β)	α rougher than β	α equal β	β rougher than α
virtual velvel/V-moving vs virtual velvet/V-static	0.49	0.19	0.32
virtual velvel/V-moving vs virtual sham/V-moving	0.52	0.15	0.33
virtual velvel/V-moving vs virtual sham/V-static	0.56	0.04	0.40
virtual velvet/V-static vs virtual sham/V-moving	0.60	0.04	0.36
virtual velvet/V-static vs virtual sham/V-static	0.31	0.17	0.52
virtual sham/V-moving vs virtual sham/V-static	0.36	0.14	0.50